Coherence limits and chirp control in long pulse free electron laser oscillator

Y. Socol, A. Gover, A. Eliran, and M. Volshonok
Department of Physical Electronics–Faculty of Engineering, Tel Aviv University, Tel-Aviv, Israel

Y. Pinhasi, B. Kapilevich, A. Yahalom, Y. Lurie, M. Kanter, M. Einat, and B. Litvak
Department of Electrical and Electronic Engineering–The College of Judea and Samaria, Ariel, Israel
(Received 26 December 2004; published 31 August 2005)

We report experimental studies of the spectral linewidth and chirp characteristics of the mm-wave rf radiation of the Israeli Electrostatic-Accelerator free electron laser (EA-FEL), along with theory and numerical simulations. The simulations, matching the experimental data, were carried out using a space-frequency-domain model. EA-FELs have the capacity to generate long pulses of tens microseconds and more, that in principle can be elongated indefinitely (cw operation). Since a cold beam FEL is by nature a ''homogeneously broadened laser,'' EA-FEL can operate, unlike other kinds of FELs, at a single longitudinal mode (single frequency). This allows the generation of very coherent radiation. The current status of the Israeli Tandem Electrostatic-Accelerator FEL, which is based on an electrostatic Van de Graaff accelerator, allows the generation of pulses of tens microseconds duration. It has been operated recently past saturation, and produced single-mode coherent radiation of record narrow inherent relative linewidth $\sim\Delta f/f = 10^{-6}$ at frequencies near 100 GHz. A frequency chirp was observed during the pulses of tens of microseconds (0.3–0.5 MHz/ms). This is essentially a drifting ''frequency-pulling effect,'' associated with the accelerator voltage drop during the pulse. Additionally, damped relaxation of the FEL oscillator was experimentally measured at the beginning and the end of the lasing pulse, in good correspondence to our theory and numerical simulations. We propose using the chirped signal of the pulsed EA-FEL for single pulse sweep spectroscopy of very fine resolution. The characteristics of this application are analyzed based on the experimental data.

DOI: 10.1103/PhysRevSTAB.8.080701 PACS numbers: 07.57.−c

I. INTRODUCTION

There is recently renewed interest in THz technologies, including imaging and spectroscopy for scientific and practical applications [1–3]. Electrostatic-accelerator free electron lasers (EA-FELs) can operate in this regime, with very high optical quality of parameters (coherence and power) of the radiation beam, and are most fitting for studying THz technologies and applications, especially in spectroscopy. These FELs have the capacity to generate long pulses of tens of microseconds and more, that in principle can be elongated indefinitely (cw operation). Since a cold beam FEL is by nature a ''homogeneously broadened laser,'' EA-FEL can operate, unlike other kinds of FELs, at a single longitudinal mode (single frequency). This allows the generation of very coherent radiation and achieving very high average power.

The Israeli Tandem Electrostatic-Accelerator FEL, which is based on an electrostatic Van de Graaff accelerator, was relocated to Ariel several years ago and returned to operation [4]. The current status allows the generation of pulses of tens of microseconds duration. The mm-wave radiation is now transmitted to the user-center rooms, where it can be utilized. A peak power of 150 W usable radiation was previously reported [4].

Here we report results of new more accurate measurements of the frequency spectrum, and increased power emission. We present calculations, matching the experimental data. Calculations were performed partly numerically using a space-frequency-domain model. Application feasibility of the controlled chirp to spectroscopy is also discussed.

II. THE EXPERIMENTAL SETUP

The EA-FEL device is shown schematically in Fig. 1, and described in detail elsewhere [4,5]. In all the described experiments, the accelerating voltage varied from 1.32 to 1.36 MV. The electron beam current though the wiggler was measured by Rogowsky coils [5] to be 1.83 A. The fast (μs-long) changes of the terminal voltage were measured by calibrated capacitive pickup probe connected to 100 MHz oscilloscope. Based on the terminal voltage drop and electron beam current measurements, the terminal capacitance was estimated as 360 ± 20 pF.

The mm-wave radiation is transported to the user's rooms by means of a corrugated overmoded waveguide. The measurements were performed by two means: (a) power measurements using a *W*-band detector Millitech −DXP-10; (b) spectral measurements using an heterodyne mixer of Hughes-47496H-100 with local oscillator (LO) from a HP-8797D network analyzer. In both cases, a Tektronix −TDS-784A oscilloscope was used to monitor the output. The input signal was attenuated in order to cope with the dynamic range of the detectors. A *W*-band down-converter, based on a waveguide mixer and stable local

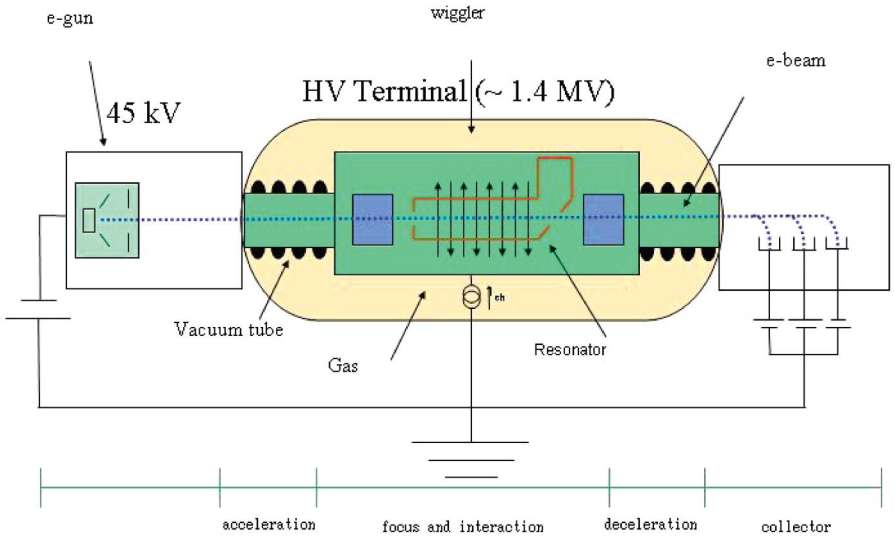

FIG. 1. (Color) Schematic drawing of the Israeli Electrostatic-Accelerator FEL configuration.

oscillator (LO), produces on the scope the difference (beat) intermediate frequency (IF):

$$f_{\mathrm{IF}} = f - f_{\mathrm{LO}} \tag{1}$$

where f_{LO} is local oscillator (LO) frequency. There is no distinction in the measurement between negative and positive frequencies, and what is seen on the oscilloscope is a signal of frequency $|f_{\mathrm{IF}}|$.

In order to obtain quantitative frequency data, we performed the so-called I/Q analysis. The obtained oscilloscope signal was multiplied by $\sin(\omega_0 t)$ and $\cos(\omega_0 t)$, with ω_0 corresponding to an arbitrary chosen frequency. These multiplied signals I and Q were subjected to low-pass filters of 15 MHz bandwidth. Then, amplitude $I^2 + Q^2$ and phase deviation $\mathrm{arctg}(Q/I)$ were extracted, and the frequency deviation $\Delta f(t) = f - f_0$ was obtained as the time derivative of the phase deviation:

$$\Delta f(t) = \frac{1}{2\pi}\frac{d}{dt}\mathrm{arctg}\left[\frac{Q(t)}{I(t)}\right]. \tag{2}$$

III. RESULTS AND DISCUSSION

A. Single-mode operation and mode hopping

Figures 2 and 3 present typical experimental data. In most measurements single-mode lasing was observed after a short period of 1 μs. This had been expected because of the ''homogeneous broadening'' nature of FEL in the cold beam regime. However, it should be mentioned that mode competition was not usually observed. I.e., at the initial 1 μs-long stage of the radiation power buildup, the radiation spectrum should be characterized rather as noisy than as multimode. Additionally to single-mode operation (Fig. 2), radiation frequency jumps during the radiation pulse were observed in some cases (Fig. 3). The modes' frequencies were uniquely identified by taking several oscillograms with different heterodyne frequencies (usually by steps of 100 MHz). One can see from the amplitude curves of the numerically filtered frequencies [Fig. 3(b)] that the first mode (85 021.5 MHz) decays when the second (83 676.5 MHz) rises.

We attribute this ''mode-hopping'' effect to large accelerating-voltage drop, as in previous works [6–8]. The voltage down-drift is due to electron beam leakage to the high voltage (HV) terminal (Fig. 1). The HV drift rate as measured by the capacitive pickup was usually ~0.7–0.9 kV/μs, resulting in 7–30 kV for the observed pulses of 10–25 μs. In the other EA-FEL experiments [6,8] similar HV drops were reported (~ 1 kV/μs). We should mention that our results were obtained with 1-stage collector. Presently undertaken installation of multistage collector [9] should considerably improve the electron transport and permit longer radiation pulses.

B. Radiation power buildup: oscillator relaxation

One can observe a distinct feature at the rising stage of each mode (Figs. 2 and 3): the frequency change rate is momentarily significantly higher. This behavior is well reproduced quantitatively by the FEL3D [10] calculation (Fig. 2). We connect this phenomenon to what is called relaxation oscillation in quantum lasers [11]. In a more general context this phenomenon may be connected also to ''load pull'' in the theory of nonlinear circuits [12]. In our case we observed damped relaxation mode (see [13], Sec. 25) due to relatively high round-trip loss of the resonator. In the previous work [7] we provided theoretical background for this effect, however the accuracy of frequency measurement was then insufficient to make quantitative comparison. In the framework of the present work we have not analyzed yet this effect beyond its successful simulation with FEL3D [see Fig. 2(d)].

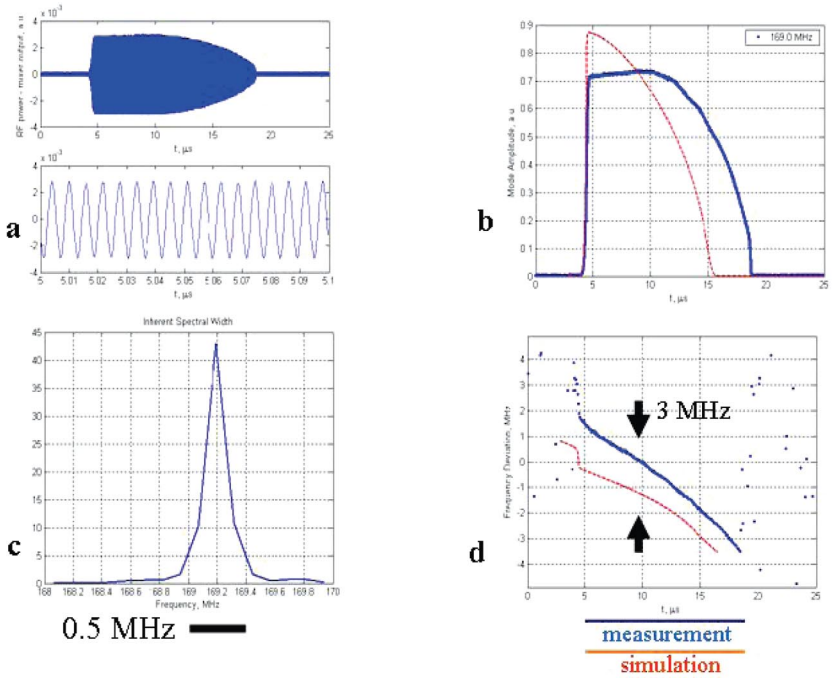

FIG. 2. (Color) Single-mode operation: (a) Original oscillogram. (b) Mode amplitude. The mode frequency is 84 401 MHz. In the I/Q analysis the low-pass filter is set to 15 MHz bandwidth. (c) Inherent spectral width after numerical elimination of the chirp (0.2 MHz). (d) Momentary frequency deviation obtained by a time derivative of the phase deviation. Data measured (continuous line) and simulated (dotted line). The chirp rate is approximately 0.35 MHz/μs in both cases.

C. Chirp analysis

In all measurements for all the identified modes, the IF signal exhibited monotonous chirp—either negative or positive (Figs. 3 and 5). For different modes within the same radiation pulse, the chirp usually had opposite signs as in Fig. 3. To determine the chirp direction of the laser signal, one should notice that if the laser signal has negative chirp (frequency drops down with time), the IF signal would also exhibit negative chirp only when $f > f_{\mathrm{LO}}$, and would exhibit a positive chirp when $f < f_{\mathrm{LO}}$ (see Fig. 4).

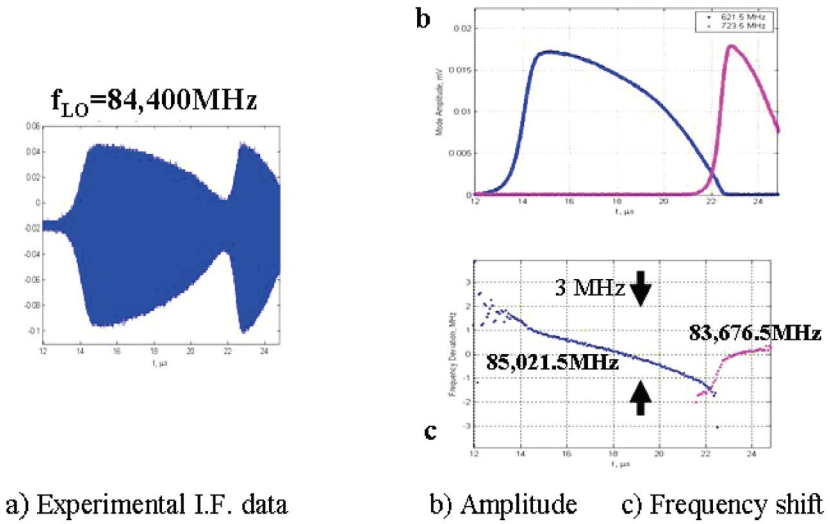

FIG. 3. (Color) Mode hopping associated with the accelerating-voltage drop: (a) IF oscillogram, (b) growth and decay of the 2 modes, (c) isolated frequency chirp measurement of the two modes (here $f_2 < f_{\mathrm{LO}} < f_1$). The chirp direction in both modes is the same (frequency decreases with time). The chirp is seen as positive for the 83 676.5 MHz mode because the mode frequency f_m, is below that of the local oscillator f_{LO} : $f_m < f_{\mathrm{LO}} = 84\,400$ MHz. Therefore the intermediate frequency $f_{\mathrm{IF}} = f_m - f_{\mathrm{LO}}$ is negative (aliasing effect). See also Fig. 4.

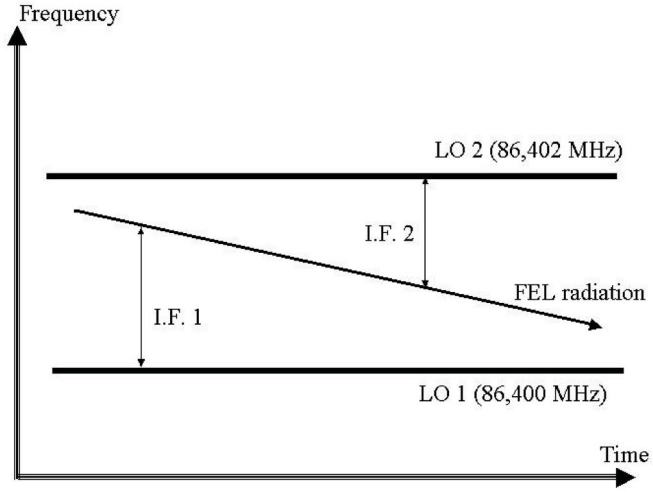

FIG. 4. Aliasing and chirp direction. If the radiation has negative chirp (frequency drops down with time), the intermediate frequency (IF) signal will exhibit negative chirp only when its frequency f is higher than that of the local oscillator (LO): $f > f_{\mathrm{LO}}$. When $f < f_{\mathrm{LO}}$ IF signal will exhibit a positive chirp.

Figure 5 shows typical oscillograms of the radiation, taken with heterodyne mixer frequency set at two close frequencies: (a) 86 400 MHz and (b) 86 402 MHz, enabling the accurate determination of the single-mode radiation frequency $f = 86\,401 \pm 1$ MHz. At heterodyne (local oscillator—LO) frequency $f_{\mathrm{LO}} = 86\,400\ \mathrm{MHz} < f$, the intermediate frequency decreases with time, and at $f_{\mathrm{LO}} = 86\,402\ \mathrm{MHz} > f$—IF increases with time. This confirms the negative direction of the laser chirp, i.e., that the radiation frequency actually decreases with time.

We associate the exhibited down-shift frequency chirp effect with the drift of the gain curve due to the beam energy drop during the pulse (see Fig. 6). The chirp can be explained then as a time varying "frequency-pulling" effect [11] of the laser oscillator. A theoretical analysis of this effect was provided in our earlier publication [7].

We analyze here the chirp effect in terms of the basic theory of frequency pulling in laser oscillators [11]. In our case this frequency-pulling shift varies with time (chirps) due to the drift of the gain curve associated with the accelerator voltage drop during the pulse (Fig. 6). Namely, for resonator eigenmode frequency f_m, resonator mode linewidth (FWHM) $\Delta f_{1/2}$, maximum-gain frequency $f_{\max}$ and gain bandwidth Δf, the pulled oscillation frequency f is given by [11]:

$$f - f_m = (f_{\max} - f_m) \cdot \Delta f_{1/2}/\Delta f. \tag{3}$$

During the pulse, $f_{\max} = f_{\max}(t)$ drifts towards lower frequencies (due to the accelerating-voltage drop) as shown in Fig. 5. The gain frequency drift rate is

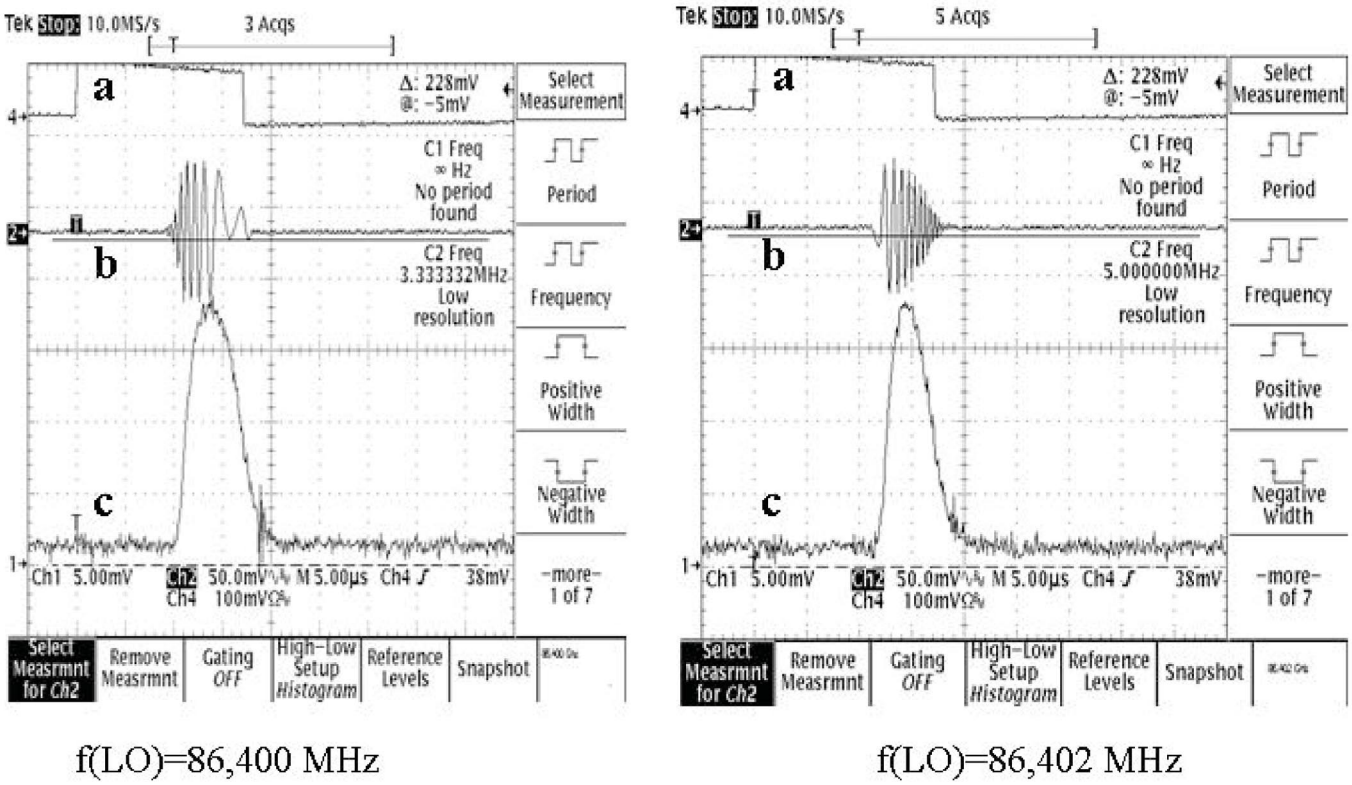

FIG. 5. Direct manifestation of the negative direction of the radiation chirp. Top trace: (*a*) *e*-beam current pulse. (*b*) heterodyne intermediate frequency (IF) output. (*c*) total *W*-band power. The local oscillator (LO) frequency f_{LO} is set very close to laser frequency: Left: $f_{\mathrm{LO}} = 86\,400$ MHz—the IF frequency decreases with time. Right: $f_{\mathrm{LO}} = 86\,402$ MHz—IF increases with time.

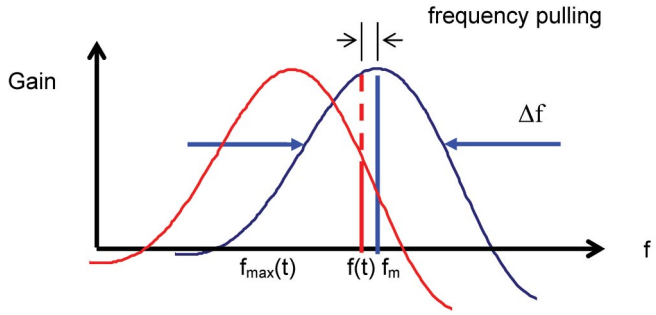

FIG. 6. (Color) The frequency-pulling effect. At $t = t_1$ (right-hand curve), it is assumed that the radiation is built up in the resonator so that the dominant mode m is excited at the maximum-gain frequency: $f_m = f_{\max}(0)$. As the gain curve shifts to lower frequencies (left-hand curve) $f_{\max}(t_2) < f_{\max}(t_1)$, there is a corresponding down-shift in the stored radiation frequency $f < f_m$ due to the frequency-pulling effect.

$$\frac{df_{\max}}{dt} = K\frac{dV}{dt}, \tag{4}$$

where

$$K = \frac{e}{mc^2}\frac{df_{\max}}{d\gamma} \tag{5}$$

is the sensitivity of the maximum-gain frequency $f_{\max}$ to voltage drop.

In a waveguide resonator the dependence of the maximum-gain frequency on beam energy is given by (see, e.g., [14]):

$$f_{\max} = \frac{\gamma_{z0}^2\beta_{z0}c}{2\pi}\left(k_w + \frac{\overline{\theta}_{\max}}{L_w}\right) \times\left[1 \pm \sqrt{\beta_{z0}^2 - \frac{(2\pi f_{co})^2}{[\gamma_{z0}(k_w + \overline{\theta}_{\max}/L_w)c]^2}}\right], \tag{6}$$

where

$\overline{\theta}_{\max}$ = the maximal gain of detuning parameter,

f_{co} = the cutoff frequency of the resonator waveguide.

This dependence is shown in Fig. 7 for the parameters of the Israeli FEL [4].

Calculating $df_{\max}/d\gamma$ from the slope of the curve in Fig. 7 we evaluated [Eq. (5)] for our operating parameters: $K = 156$ MHz/kV. The FWHM bandwidth of the FEL gain Δf was calculated using the FEL3D code that performs 3D solution of particle motion equations coupled to Maxwell equations, using a space-frequency domain model. The calculations yielded $\Delta f = 6.0$ GHz. The resonator eigenmode linewidth $\Delta f_{1/2}$ was measured (in the "cold" resonator) to be $\Delta f_{1/2} = f_0/Q \sim 17$ MHz (Q factor of 5×10^3 at 86 GHz). The voltage drop rate was measured to be 0.7 kV/μS. The model-calculated chirp rate [Eq. (3)] is therefore $df/dt = 0.3$ MHz/μs.

This value is in excellent correspondence with the experimental data, taking into account the accuracy of the

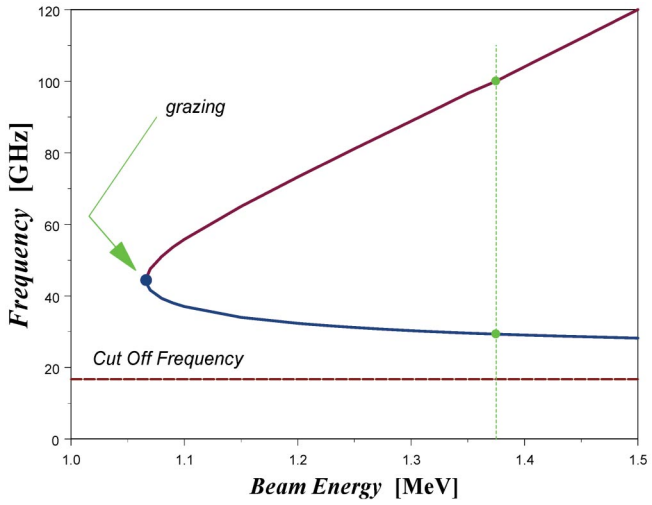

FIG. 7. (Color) Israeli FEL frequency dependence on the beam accelerating energy $(\gamma\text{–}1)$ mc^2.

parameters involved in the calculation. The experimentally measured chirp behavior agrees well also with results of FEL3D simulation (see Fig. 2). The simulated instantaneous frequency (dashed curve) was calculated by evaluating the rate of phase accumulation change in each round-trip traversal of the oscillation buildup [10]. The beam energy γ at each traversal was updated in the code in accordance to the measured voltage drop rate 0.7 kV/μs.

D. Inherent spectral width

We define the inherent spectral width of the laser radiation as the linewidth of the wave when the spectral broadening due to the chirp is eliminated. To obtain the inherent spectral width we performed a linear time-stretching transformation $t' = t(1 + tf_1/f_0)$. This eliminates the chirp from the chirped signal: $\sin[(\omega_0 + \omega_1 t)t] = \sin(\omega_0 t')$. The chirp rate parameter used was $f_1 = 0.35$ MHz/μs as follows from the slope of the experimental curve in Fig. 2. The Fourier spectrum of the transformed signal is shown in Fig. 2(c), exhibiting an inherent spectral linewidth (FWHM) of 0.2 MHz (in comparison with 2.0 MHz FWHM of the original chirped signal spectrum). The spectrum width is somewhat higher than the pulse-duration-limited value (0.1 MHz) because the actual chirp is slightly nonlinear in time in the end of the pulse. The measured linewidth value of $\Delta f/f \cong 2 \times 10^{-6}$ is to our knowledge a record narrow linewidth that was recorded so far with FEL. Based on the theory of [7], narrower inherent linewidth value would be possible with planned longer pulse operation, which would allow very high resolution single pulse spectroscopy, as discussed in the next section.

In Fig. 8 we show a different processing of the IF data. A spectrogram in ω-t phase space was computed by employing a running window Fourier transform [7] of 1 μs width. This window makes it possible to observe the spectrum chirp, which agrees well with the 0.35 MHz/μs estimate,

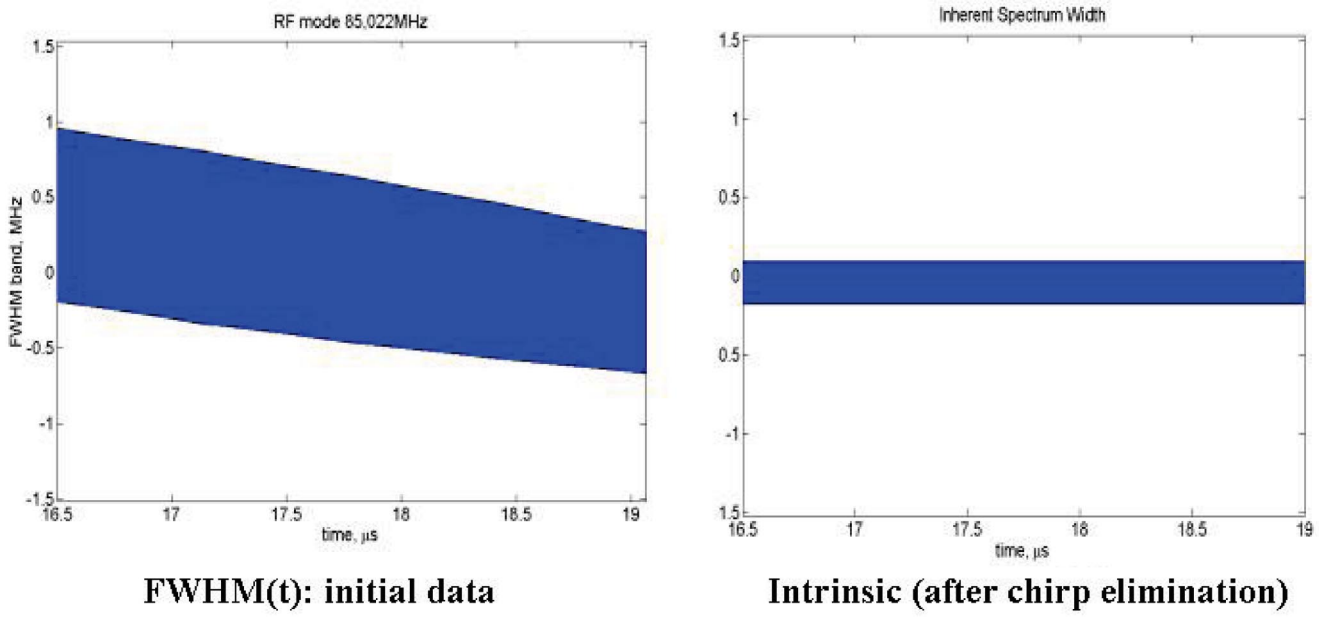

FIG. 8. (Color) Spectral FWHM of a rf mode. Local oscillator frequency is 85 022 MHz. Left: initial data; right: after the digital chirp elimination. Time window is 1 and 10 μs correspondingly.

but the short time window limits the measurable bandwidth to 1 MHz $= 1\ \mu s^{-1}$. We then eliminated the chirp digitally by applying on the recorded data the time-stretching transformation described earlier, and used a window of 10 μs to obtain the spectrogram of Fig. 8 (right). In this case, the bandwidth is window limited to 0.1 MHz, enabling the determination of the ''inherent'' mode linewidth as 0.27 MHz.

E. Single pulse sweep spectroscopic applications

Since EA-FEL produces an intense long pulse radiation of extremely high inherent spectral purity, it may be used for spectroscopic applications. An interesting possibility is to perform single pulse spectroscopy—namely, to use the radiation chirp as a frequency sweeper (Fig. 9). Let us estimate the feasible parameters for such an application.

For spectroscopic application there are two crucial parameters: sweep range and spectral resolution. The sweep range depends on the frequency-pulling effect process. Based on Eq. (3) (see Fig. 9), the sweep (uniform chirp) range is

$$\Delta f_{\text{sweep}} = \Delta f_{\text{hop}} \Delta f_{1/2} / \Delta f, \tag{7}$$

where the cold resonator FWHM linewidth is given for a Fabri-Perot resonator (see Ref. [11]; the notation is different there) by

$$\Delta f_{1/2} \approx \Delta f_{\text{FSR}} (1 - R_{rt}) / 2\pi \tag{8}$$

Δf_{FSR} is the free spectral range between the modes of the resonator, and we assumed $1 - R_{rt} \ll 1$ (R_{rt} is the round-trip reflectivity factor of the resonator including losses and out-coupling factors). The parameter Δf_{hop}

$$\Delta f_{\text{hop}} = \Delta f_{\max} - f|_{g=1-R} \tag{9}$$

is the range of permissible shift of the FEL gain curve during the lasing pulse during which the lasing condition $g = (P_{\text{out}} - P_{\text{in}})/P_{\text{in}} > 1 - R$ is retained, and beyond which the laser would hop to lase at a different resonator mode or cease lasing altogether. Clearly (see Fig. 9), this range is

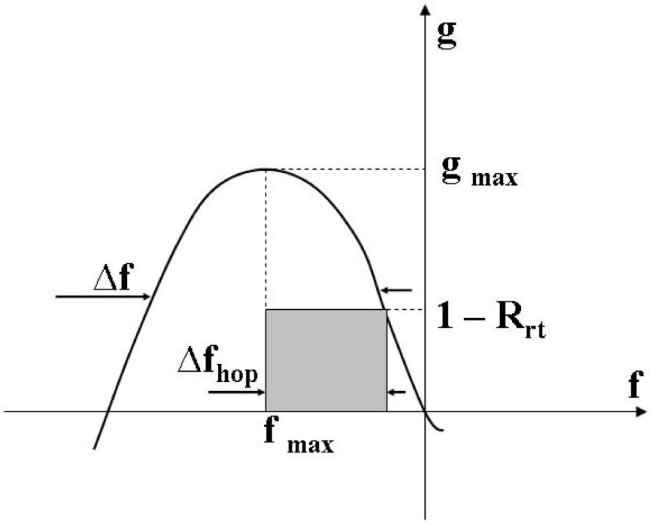

FIG. 9. Frequency shift Δf_{hop} is the range in which the lasing condition $g > 1 - R_{rt}$ is retained. Beyond this limit the laser would hop to lase at a different resonator mode or cease lasing altogether. This range is longer the higher is the gain and the lower is the factor $1 - R_{rt}$. The optimal value of $1 - R_{rt}$ maximizing Δf_{sweep} corresponds to a state of maximal area of the shaded rectangle.

longer the higher is the gain and the lower is the factor $1–R_{rt}$. On the other hand the resonator mode linewidth $\Delta f_{1/2}$ [Eq. (8)] is growing in proportion to $(1–R_{rt})$. Evidently there is an optimal value of $1–R_{rt}$ for which Δf_{sweep} [Eq. (7)] can be maximized (in Fig. 9 it corresponds to a state of maximal area of the shaded rectangle).

In Fig. 10 we present the scaling of Δf_{sweep} as a function of the maximum gain $g_{\max}$ of the FEL, assuming operating in the low gain regime ($g < 1$). The free spectral range used was the experimentally measured $\Delta f_{\text{FSR}} = 115$ MHz. Note that the experimentally measured chirp range ~3 MHz [see Fig. 2(d)] falls within the sweep range estimated in Fig. 10.

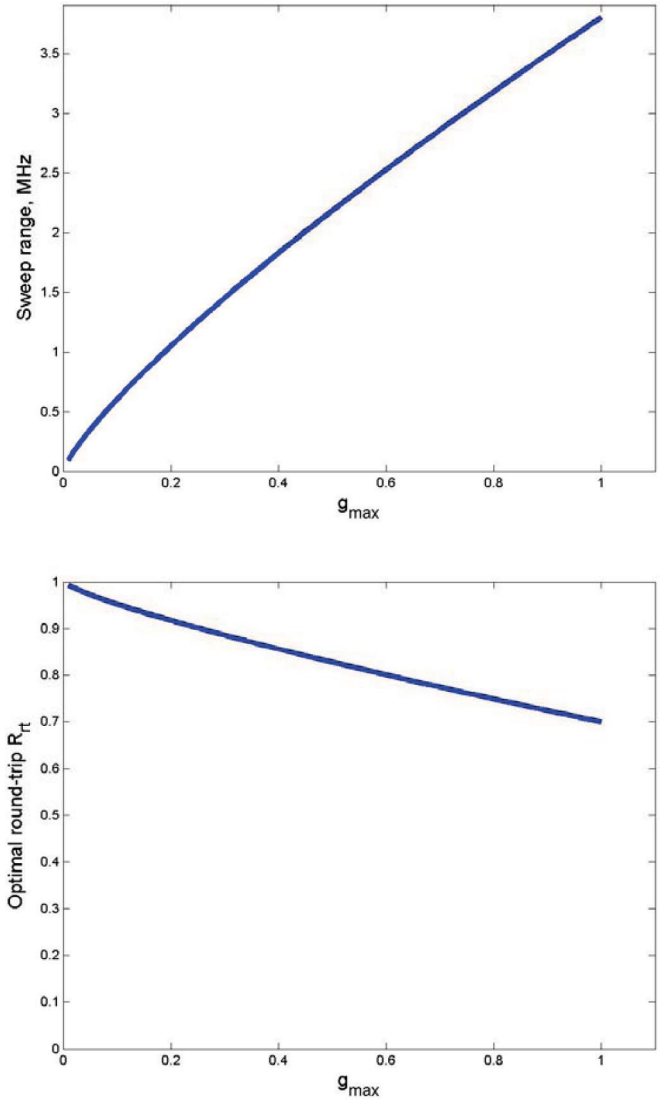

FIG. 10. (Color) The scaling of Δf_{sweep} and optimal round-trip reflectivity R_{rt} as functions of the maximum gain $g_{\max}$ of the FEL $g = (P_{\text{out}}–P_{\text{in}})/P_{\text{in}}$, assuming operating in the low gain regime ($g < 1$). The free spectral range used was the experimental measured $\Delta f_{\text{FSR}} = 115$ MHz. Note that the experimentally measured chirp range ~3 MHz [see Fig. 2(d)] falls within the estimated sweep range.

The other important parameter for spectroscopic application is the spectral resolution. Here we distinguish between coherent and incoherent detection of the chirped FEL radiation signal and the transmitted signal. In Fig. 11(a) the detection process is described in time-frequency phase space. The center frequency of the coherent radiation pulse $E_i(t)$ is chirped during the pulse time t_p:

$$f(t) = f_0–f_1 t, \tag{10}$$

where $f_1 = \Delta f_{\text{sweep}}/t_p$ is the chirp rate. The momentary spectral width of the FEL radiation is very narrow, assumed to be Fourier transform limited:

$$\Delta f_{\text{inh}} = 1/t_p. \tag{11}$$

When the FEL chirped radiation pulse is transmitted through an optical sample of complex transmission factor $t(f)$ and the optical power is detected (incoherent detection), the time dependence of the detected power replicates the transmission spectrum of the sample $t(f)$ [Figs. 11(a) and 11(b)]. If we want to resolve a transmission line of width δf_{res} the sweep rate must be slow enough so that the sweep time through the transmission line $\delta t = f_1 \delta f_{\text{res}}$ will be long (steady state approximation) relative to the polarization decay time $1/\delta f_{\text{res}}$ of the transmitted signal. This sets a limit on the spectral resolution for incoherent detection:

$$\delta f_{\text{res}} = \sqrt{f_1} = \sqrt{(\Delta f_{\text{sweep}}/t_p)}. \tag{12}$$

We can take advantage of our ability to detect coherently both the FEL incoming signal and the transmitted signal using heterodyne detection as described before [Fig. 11(c)]. Having the full recorded data (amplitude and phase) of $E_i(t)$ and $E_0(t)$, the full (complex) value of the transmission factor $t(f)$ can be restored after Fourier transformation $\boldsymbol{F}\{\,\}$ of the recorded signals

$$t(f) = \boldsymbol{F}\{E_o(t)\}/\boldsymbol{F}\{E_i(t)\}. \tag{13}$$

The spectral resolution in this case is Fourier transform limited and given by the inherent linewidth value

$$\Delta f_{\text{res}} = 1/t_p. \tag{14}$$

Table I lists resolution limits for a sweep range of 5 MHz and several planned values of pulse duration for both the incoherent and coherent schemes.

IV. CONCLUSIONS

Electrostatic-accelerator FELs are capable of operating with extremely narrow Schawlow-Townes fundamental linewidth [15]. We have measured record narrow inherent (eliminating chirp-broadening) relative linewidth $-\Delta f/f \approx 10^{-6}$ at frequencies near 100 GHz with the Israeli EA-FEL. A frequency chirp of 0.3–0.5 MHz/μs

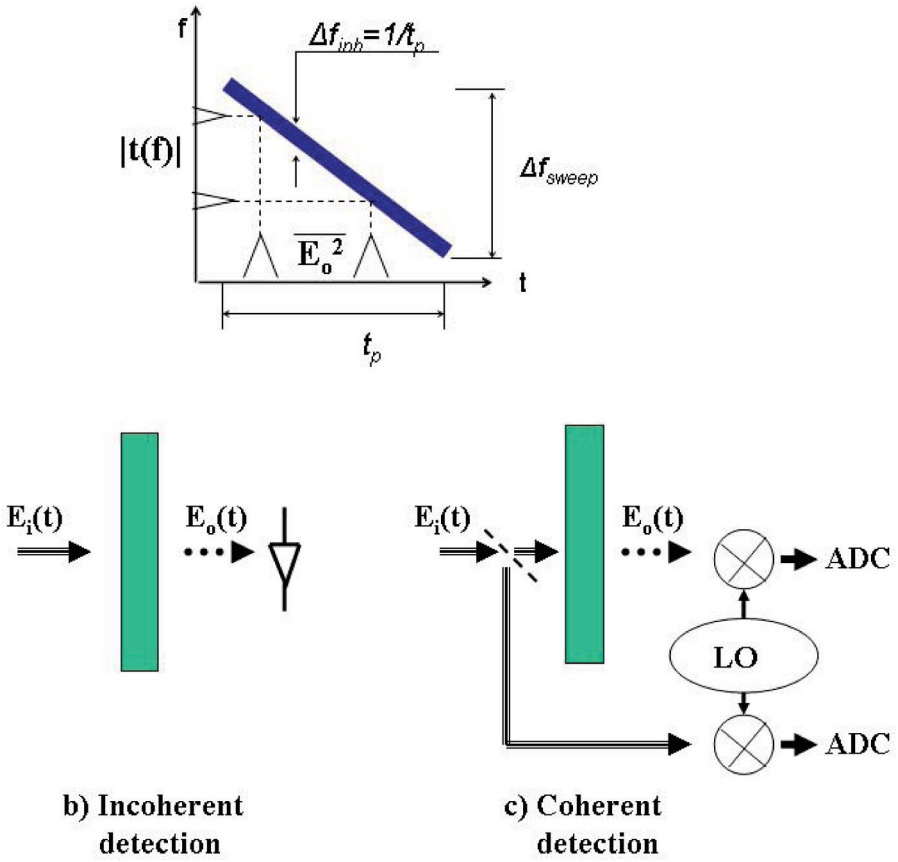

FIG. 11. (Color) (a) The detection process in time-frequency phase space. The center frequency of the coherent radiation pulse $E_i(t)$ is chirped during the pulse time t_p : $f(t) = f_0 – f_1 t, f_1 = \Delta f_{\text{sweep}}/t_p$ is the chirp rate. (b) Incoherent detection—the spectral resolution is low (see Table I). (c) Coherent detection. LO is local oscillator, ADC is analog-to-digital converter. The spectral resolution is pulse-time Fourier limited.

TABLE I. Resolution limits for sweep range 5 MHz and several pulse times. For coherent measurements, the resolution is limited by the inherent linewidth. For incoherent, it is considerably worse and scales as inverse square root of the pulse duration.

Pulse time, μs	Sweep rate f', MHz/μs Sweep range: 5 MHz	Resolution δf_{res}, kHz Coherent (complex)	Incoherent (scalar)
10	0.5	100	700
100	0.05	10	200
1000	0.005	1	70

was observed during pulses of 10–25 μs duration. This effect is associated with the accelerator voltage drop during the pulse and is interpreted as a consequent drifting frequency-pulling effect. Frequency instability effects at the onset of the oscillation (relaxation, load pull) were also observed and interpreted based on numerical simulations. We suggest that with further development of the FEL, the chirp effect can be controlled and be used in single pulse spectroscopy, providing at mm and THz frequencies a sweep range of about 10 MHz with resolution as low as 1 kHz ($\Delta f/f = 10^{-8}$) with a 1 ms long pulse.

ACKNOWLEDGMENTS

This work was carried out at the Israeli FEL National Knowledge Center supported by the Ministry of Science and Technology, Israel.

[1] Z. Jiang *et al.*, Appl. Phys. Lett. **76**, 3221 (2000).
[2] B. Ferguson and X. C. Zhang, Nat. Mater. **1**, 26 (2002).
[3] *THz Imaging and Sensing for Security Applications*, Proc. SPIE Int. Soc. Opt. Eng. Vol. 5070, edited by R. L. Hwu

and D. L. Woolard (SPIE-International Society for Optical Engineering, Bellingham, WA, 2003).
[4] A. Gover *et al.*, Nucl. Instrum. Methods Phys. Res., Sect. A **528**, 23 (2004).
[5] A. Abramovich *et al.*, Nucl. Instrum. Methods Phys. Res., Sect. A **407**, 16 (1998).
[6] B. G. Danly *et al.*, Phys. Rev. Lett. **65**, 2251 (1990).
[7] A. Abramovich *et al.*, Phys. Rev. Lett. **82**, 5257 (1999).
[8] W. H. Urbanus *et al.*, Phys. Rev. Lett. **89**, 214801 (2002).
[9] A. Gover *et al.*, in Proceedings of the FEL2005 Conference, SLAC (to be published).
[10] Y. Pinhasi, Int. J. Electron. **78**, 581 (1995).
[11] A. Yariv, *Optical Electronics* (Holt Rinehart and Winston, Austin, TX, 1985), 3rd ed., Sec. 6.2-5.
[12] Y. Itoh and K. Honjo, IEICE Trans. Electron. **E86C**, 108 (2003).
[13] L. D. Landau and E. M. Lifshitz, *Mechanics* (Butterworth-Heinemann, Oxford, 2003), 3rd ed.
[14] E. Jerby and A. Gover, IEEE J. Quantum Electron. **21**, 1041 (1985).
[15] A. Gover, A. Amir, and L. R. Elias, Phys. Rev. A **35**, 164 (1987).